Helix Bending in Alamethicin: Molecular Dynamics Simulations and Amide Hydrogen Exchange in Methanol

Nick Gibbs, Richard B. Sessions, Philip B. Williams, and Christopher E. Dempsey
Biochemistry Department and Centre for Molecular Recognition, Bristol University, Bristol BS8 1TD, England

ABSTRACT Molecular dynamics simulations of alamethicin in methanol were carried out with either a regular α-helical conformation or the x-ray crystal structure as starting structures. The structures rapidly converged to a well-defined hydrogen-bonding pattern with mixed α-helical and 3_{10}-helical hydrogen bonds, consistent with NMR structural characterization, and did not unfold throughout the 1-ns simulation, despite some sizable backbone fluctuations involving reversible breaking of helical hydrogen bonds. Bending of the helical structure around residues Aib10-Aib13 was associated with reversible flips of the peptide bonds involving G11 (Aib10-G11 or G11-L12 peptide bonds), yielding discrete structural states in which the Aib10 carbonyl or (rarely) the G11 carbonyl was oriented away from the peptide helix. These peptide bond reversals could be accommodated without greatly perturbing the adjacent helical structure, and intramolecular hydrogen bonding was generally maintained in bent states through the formation of new (non-α or 3_{10}) hydrogen bonds with good geometries: G11 NH-V9 CO (inverse γ turn), Aib13 NH-Aib8 CO (π-helix) and, rarely, L12 NH- Q7 NH (π-helix). These observations may reconcile potentially conflicting NMR structural information for alamethicin in methanol, in which evidence for conformational flexibility in the peptide sequence before P14 (G11-Aib13) contrasts with the stability of backbone amide NH groups to exchange with solvent. Similar reversible reorientation of the Thr11-Gly12 peptide bond of melittin is also observed in dynamics simulations in methanol (R. B. Sessions, N. Gibbs, and C. E. Dempsey, submitted). This phenomenon may have some role in the orientation of the peptide carbonyl in solvating the channel lumen in membrane ion channel states of these peptides.

INTRODUCTION

Alamethicin is one of the most widely studied examples of a class of polypeptides from microorganisms and animal venoms that diffuse into membranes as amphipathic α-helices and induce voltage-gated ion conductance (Woolley and Wallace, 1992; Sansom, 1993; Cafiso, 1994). Conducting channels are composed of transmembrane associations of helical monomers in a "barrel" array surrounding an aqueous lumen through which ions permeate. The pores are formed by voltage-induced transitions from "pre-pore" states by mechanisms that are incompletely characterized. The voltage-induced transitions must involve interaction with the peptide helix dipole, because the Q18 variant of alamethicin, having no fixed charges, is active. (The amino acid sequence of the alamethicin variant used here is Ac-U-P-U-A-U-A-Q-U-V-U-G-L-U-P-V-U-U-Q-Q-Phol, where U is the one-letter code for α-aminoisobutyric acid (also abbreviated here as Aib) (Sansom, 1993), Ac is acetyl, and Phol is phenylalaninol.) This has led to consideration of the role of the proline 14 residue, which is expected to disrupt helical structure near the center of the peptide sequence. Some models of voltage-induced transitions from "pre-pore" to conducting channel states propose the augmentation of the helix dipole by transition of bent or C-terminally disrupted conformations to more regular helical conformations as a "voltage sensor." Calculations indicate that conformational transitions involving augmentation of the helix dipole cannot account for the full gating charge (Sansom, 1993), but may make some contribution to voltage gating; bending around the P14 residue may also contribute to channel stabilization (Dempsey et al., 1991; Duclohier et al., 1992) and to channel noise (Mak and Webb, 1995).

Although recent studies have been aimed at characterizing the structural properties of alamethicin in membranes (Brumfeld and Miller, 1990; Woolley and Wallace, 1993; North et al., 1995; He et al., 1996; Dempsey and Handcock, 1996), the most detailed information on the conformational properties of alamethicin have come from NMR studies of the peptide in methanol. Although it is clear that the peptide adopts an essentially helical conformation in methanol, conflicting conclusions about the effect of the P14 residue on helix structure and stability have been made. ^{13}C NMR relaxation rates (Kelsh et al., 1992) and amide hydrogen exchange measurements (Dempsey, 1995) indicate that the alamethicin helix is rather stable in methanol, with little perturbation of hydrogen bonding around the P14 residue, although mixed α- and 3_{10}-helical hydrogen bonding is required to accommodate the proline. Proton relaxation measurements in a C-terminally spin-labeled analog, and detailed analysis of NMR distance constraints, amide NH temperature coefficients, and ^{1}H, ^{13}C, and ^{15}N chemical shifts have indicated, respectively, bent conformations

Received for publication 17 December 1996 and in final form 19 March 1997.

Address reprint requests to Dr. C. E. Dempsey, Department of Biochemistry, School of Medical Sciences, Bristol University, University Walk, Bristol BS8 1TD, England. Tel.: 0-117-9287569; Fax: 0-117-9288274; E-mail: dempsey@bsa.bristol.ac.uk.

Dr. Williams' present address is School of Biology and Biochemistry, University of Bath, Claverton Down, Bath, England.

0006-3495/97/06/2490/06 $2.00

(North et al., 1994) and conformational flexibility around residues G11-L12 (Yee et al., 1995). As part of a study to determine the extent to which molecular dynamics simulations can yield insight into the backbone fluctuations in helical polypeptides that underlie amide exchange, we have carried out dynamics simulations on alamethicin solvated in methanol, using both a regular α-helical conformation and the x-ray crystal structure (Fox and Richards, 1982) as starting structures. We find that both simulations evolve rapidly into a similar, largely α-helical, conformation containing some 3_{10}-helical hydrogen bonds consistent with NMR (Esposito et al., 1987; Yee and O'Neil, 1992; Yee et al., 1995) and amide exchange data (Dempsey, 1995). The peptide undergoes bending motions associated with discrete flips of the ϕ and ψ torsion angles around the peptide bonds involving G11. Despite this perturbation of helical structure, stable hydrogen bonding can be maintained, partly through the formation of nonregular (i.e., not α or 3_{10}) hydrogen bonds. The structural properties of alamethicin observed in the solvated dynamics simulations may provide a rationalization of several conflicting pieces of structural information obtained in the NMR studies.

MATERIALS AND METHODS

General simulation conditions

Molecular mechanics calculations were carried out using DISCOVER 2.95 (Biosym Technologies) with the CVFF force field (Dauber-Osguthorpe et al., 1988), and dynamics trajectories were analyzed using FOCUS (Sessions et al., 1989; Osguthorpe and Dauber-Osguthorpe, 1992). Molecular mechanics calculations were carried out using minimum image periodic boundary conditions at constant volume. Nonbonded electrostatic and van der Waals forces were truncated at a 12-Å radius via a smoothing function over 2 Å. Structure inspection and analysis was carried out using InsightII (Biosym Technologies).

Solvent generation

The unit cell of the crystal structure of methanol at −110°C (Tauer and Lipscomb, 1952) was replicated (5 × A, 4 × B, 7 × C) to generate 560 molecules. Partial charges for the methanol atoms were [H3 (0.00), C (0.10), O (−0.35), H (0.25)], based on semiempirical molecular orbital calculations of an isolated molecule (MOPAC, AMI and PM3 Hamiltonians). The orientation of the methanol molecules in the solvent box was randomized by performing 50 ps of molecular dynamics under periodic boundary conditions with cell dimensions of 34 × 34 × 34 Å at 300 K. The resulting density of methanol of 0.76 g/cm^3 is close to the experimental value of 0.79 g/cm^3 at room temperature. This solvent box was used in the soaking procedure described below.

Peptide construction and refinement

A right-handed 20-residue polyalanine α-helix was constructed and "mutated" into the alamethicin sequence. Intramolecular van der Waals overlaps of 30% or more were removed by manual adjustment of the side-chain torsion angles. Inevitable clashes between the proline residues and the surrounding sequences were ignored at this stage, because these could not be altered without disrupting the α-helical conformation. Molecule A from the unit cell of the alamethicin x-ray structure (Fox and Richards, 1982; Protein Data Base code 1ALM) was used as a starting structure for one simulation. The structures were centered in unit cells (50 × 33 × 33 Å), with the helix axis oriented parallel to the longest side of the box. Each system was solvated in methanol, resulting in an even distribution of 675 molecules surrounding the peptide.

Energy minimization

Before dynamics simulations, the peptide/solvent ensembles were energy minimized according to the following protocol. Initially the solvent alone was relaxed around the peptide. The peptide was then allowed to relax under tethering constraints. Finally, this constraint was removed and the whole ensemble was subjected to 4000 cycles of conjugate gradient minimization.

Molecular dynamics

The simulations were initialized by assigning random velocities to all atoms with a Boltzman distribution consistent with a temperature of 300K. Integration over time was performed with the Verlet algorithm and a time step of 1 fs. Coordinates were saved every 0.1 ps for analysis.

Percentage hydrogen bond lifetimes

Experimental percentage hydrogen bond lifetimes were calculated from amide exchange protection factors (Dempsey, 1995) as described (Dempsey et al., 1991). The calculated percentage lifetime is the proportion of the dynamics trajectory in which hydrogen bond donors and acceptors satisfy both distance (2.7 or 3.0 Å) and angle (N-H · · · O angle = 180 ± 60°) (Baker and Hubbard, 1984) criteria.

RESULTS AND DISCUSSION

The backbone conformation quickly relaxed in both simulations (α-helical or x-ray starting structures) to one that was largely α-helical with some 3_{10} hydrogen bonding. Unless otherwise stated, the data presented are from the simulation starting from α-helical conformation. The structures did not unfold during the simulations (consistent with the known properties of the peptide in methanol), and are still "native-like" after 1 ns, despite some large-amplitude structural fluctuations involving reversible breaking of hydrogen bonds (R. B. Sessions, N. Gibbs, and C. E. Dempsey, submitted). 3_{10} hydrogen bonds involving Aib3 NH (N-terminal acetyl carbonyl H bond acceptor), A4 NH, V9 NH, V15 NH, and Q18 NH were highly populated in both simulations; these residues exclusively (U3 NH, V15 NH), or almost exclusively, made 3_{10} rather than α hydrogen bonds. Relaxation to this hydrogen-bonding pattern requires only small deviations from α-helical conformation, and took place in the first few picoseconds of the simulations. The formation of mixed α and 3_{10} hydrogen-bonded structure is a response to the structural requirements for the accommodation of Aib (Marshall et al., 1990; Zhang and Hermans, 1994) and Pro (Piela et al., 1987; Barlow and Thornton, 1988; Yun et al., 1991) in helical conformation, and the promotion of intramolecular hydrogen bonds (rather than peptide-solvent hydrogen bonds) in methanol. The presence of 3_{10} hydrogen bonds involving amide NHs of residues 3 and 15 have been inferred from solution NMR studies (from the high stabilities of these NHs to exchange

with solvent (Dempsey, 1995) and the small temperature dependencies of the amide ^{1}H chemical shift (Yee et al., 1995)). A 3_{10} hydrogen bond involving V15 NH is found in the crystal structure of alamethicin crystallized from methanol (Fox and Richards, 1982), together with other, incompletely populated, 3_{10} hydrogen bonds (involving amide NHs of residues 12, 13, 18, and 19).

The most prominant deviations from helical structure were flips of backbone torsion angles involving residues Aib10, G11, and L12 (Fig. 1). Associated with these torsion flips was the loss of regular helical hydrogen bonding (α or 3_{10} H bonds) for G11 and L12 NH, and in some cases significant bending of the peptide backbone defined by the angle between helical segments N- and C-terminal to P14. The torsional flips were associated with transitions between

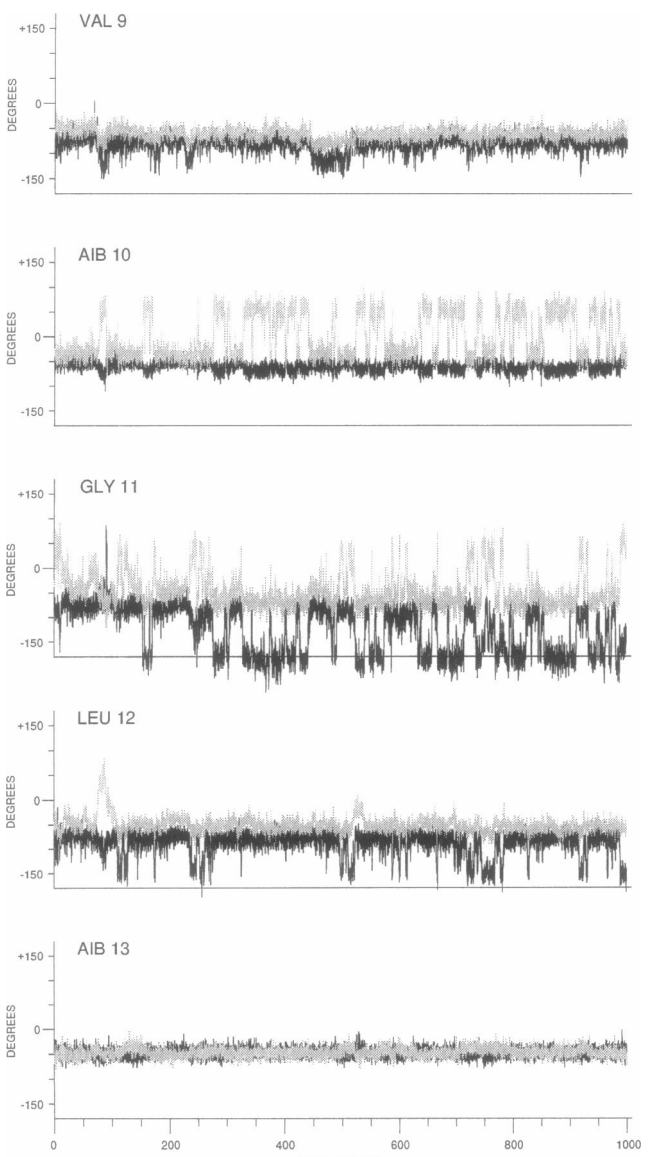

FIGURE 1 Variation of the peptide ϕ (*heavy lines*) and ψ (*light lines*) torsion angles for residues 9–13 during 1-ns molecular dynamics simulation in methanol with a regular α-helical starting structure.

three conformational states characterized by discrete ϕ and ψ torsion angle ranges for peptide bonds between Aib10 and G11, and between G11 and L12 (Table 1). Representative structures of each of these states are shown in Fig. 2. State 1 (comprising ~45% of the trajectory from the α-helical starting structure) has largely normal helical geometry; in state 2 (~50%) the Aib10-G11 peptide bond is rotated by ~90° (the carbonyl O of Aib10 faces the solvent and the G11 NH is directed into the peptide structure); state 3 (less than 5%) has a similar rotation around the G11, L12 peptide bond. The orientation of the Aib10-G11 peptide bond in the predominant states 1 and 2 (>95% of the α-helical dynamics trajectory) are shown in more detail in Fig. 3.

The perturbations of regular helical structure between Aib10 and Aib13 in states 2 and 3 is expected to result in some loss of helical hydrogen bonding. We calculated the proportion of the total trajectories in which each amide NH group makes a helical hydrogen bond either with α-helix or 3_{10}-helix carbonyl partners, and defined this parameter as the calculated "percentage lifetime." The values for residues around P14 (Aib10 NH to Aib16 NH) are listed in Table 2 (columns 1 and 2) for hydrogen bond distance constraints (H-O) of 2.7 and 3.0 Å. A separation of 2.7 Å is larger than the value (2.5 Å) normally considered the upper limit for a hydrogen bond (Baker and Hubbard, 1984), but is used to accommodate thermal motions of 0.4–0.5 Å, which can produce small transient excursions over the 2.5-Å limit that cannot be considered hydrogen-bond-breaking fluctuations. The 3.0-Å constraint is included for comparison with amide exchange data in the expectation that many of the fluctuations observed in simulations that are of very small amplitude (H-O distance up to 3.0 Å) may not be sufficient to allow exchange to occur. The "percentage lifetimes" for alamethicin in methanol calculated from amide exchange measurements are greater than 98% for residues 10–16 inclusive (Dempsey, 1995). In light of the poor knowledge

TABLE 1 Peptide backbone torsion angles for conformational states of alamethicin from dynamics trajectories

	ϕ	ψ
State 1		
U10	−50	−50
G11	−60	−45
L12	−60	−45
U13	−50	−50
State 2*		
U10	−50	+50
G11	−180	−50
State 3*		
G11	−50	+50
L12	−133	−70

* Unlisted residues have the same ϕ and ψ torsion values as state 1; the torsion angles for all other nonproline residues except Phol 20 were generally in the acceptable range for helical (α or 3_{10}) geometry in all conformational states.

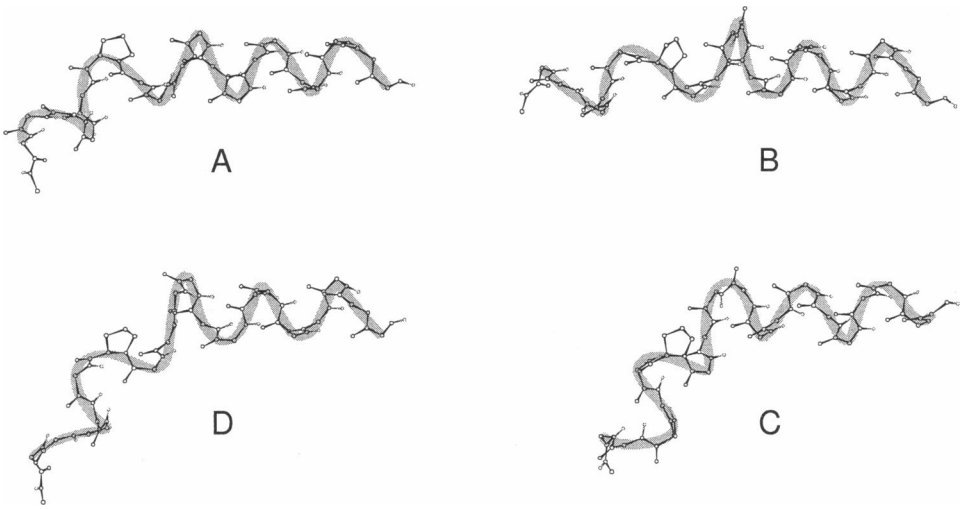

FIGURE 2 Representative backbone traces of the three conformational states of alamethicin defined by ϕ and ψ torsions around the Aib10-G11 and G11-L12 peptide bonds (see Table 1) during molecular dynamics simulation in methanol. State 1 (*A*, 930 ps) has normal helical geometry. Two state 2 structures (*B*, 289 ps; *C*, 770 ps) have a rotation around the Aib10-Gly11 peptide bond, and the state 3 structure (*D*, 750 ps) has a rotation around the Gly11-L12 peptide bond.

of the time scale and amplitude of structural fluctuations of hydrogen-bonded polypeptide structure that underlie amide exchange, quantitative agreement between experimental and simulated percentage lifetimes is not expected. However, the amide exchange data indicate that amides of residues Aib10–Aib16 form stable hydrogen bonds (none of these residues show significantly decreased experimental "percentage lifetimes"). On the other hand, G11 NH and Aib13 NH form regular helical hydrogen bonds during only a small portion of the trajectories in the simulations.

Analysis of the hydrogen-bonding patterns in states 2 and 3 containing partially reversed peptide bonds reveals two highly populated hydrogen bonds not normally observed in peptide helices. In state 2, G11 forms a stable hydrogen bond with V9 carbonyl (inverse γ turn, in which Gly is often found in the position of hydrogen bond donor; Rose et al., 1985), and in state 2 and sometimes states 1 and 3, Aib13 NH forms a stable hydrogen bond with Aib8 NH (π-helix type). These hydrogen bonds are illustrated in Fig. 3 for a representative state 2 structure occurring at 390 ps in the α-helical simulation. A π-type hydrogen bond is also sometimes found in state 2, involving L12 NH and Q7 carbonyl. With a 3-Å distance constraint, these hydrogen bonds are formed in 42% (G11 NH-V9 CO), 14% (L12 NH-Q7 CO), and 50% (Aib13 NH-Aib8 CO), respectively, of the total trajectory. If these hydrogen bonds are included in the analysis of total simulated percentage lifetimes (Table 2, columns 3 and 4), a relatively flat distribution of lifetimes is obtained for residues Aib10–Aib16 NH, indicating that each of these amides participates in hydrogen-bonded secondary structure throughout most of the simulation. Apart from the low-amplitude, high-frequency fluctuations that produce only small deviations from acceptable hydrogen bond geometry, and rare, large-amplitude reversible structural fluctuations involving concerted breaking of several hydrogen bonds, hydrogen bonding extends from the Aib3 NH at the N-terminus to Q19 NH at the C-terminus over the 1-ns simulation (R. B. Sessions, N. Gibbs, and C. E. Dempsey, submitted). This is consistent with the stable hydrogen bonding of these residues inferred from their stabilities with respect to exchange with solvent (Dempsey, 1995). A strong contribution to the overall stability of the alamethicin structure is the resistance of peptide bonds involving Aib residues to deviations from helical geometry; with the notable exception of Aib10, adjacent to a glycine, the Aib residues exhibited a rather flat distribution of peptide ϕ and ψ torsion

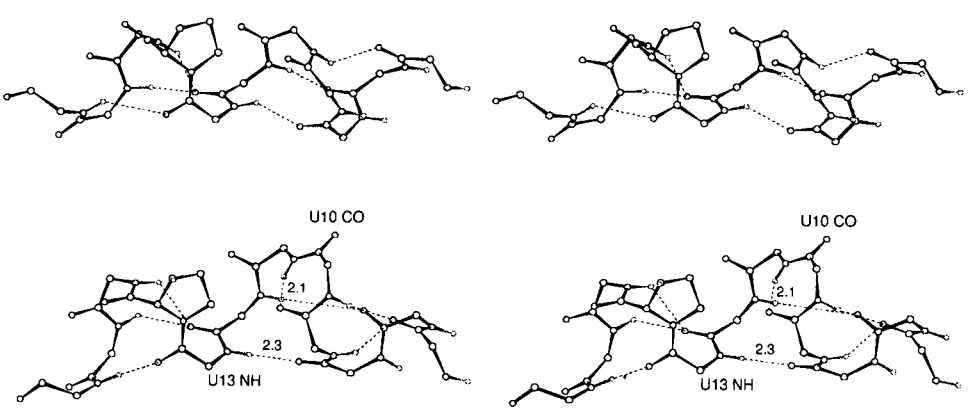

FIGURE 3 Stereo figure of representative state 1 (*top*, 440 ps) and state 2 (*bottom*, 390 ps) structures, illustrating the formation of G11-V9 and Aib13-Aib8 hydrogen bonds described in the text. The structures are extracted directly from the simulation trajectories and are not energy minimized, yielding long hydrogen bonds in some cases (see text). Annotated hydrogen bond distances are in angstroms.

TABLE 2 Percentage hydrogen bond lifetimes for amide NHs of residues 10–16 from dynamics trajectories

	Lifetime ($\alpha/3_{10}$)* %		Lifetime (total)# %	
Residue	2.7 Å	3.0 Å	2.7 Å	3.0 Å
Aib10	79.6	87.3	79.6	87.3
Gly11	40.2	48.0	82.02	90.1
Leu12	52.5	67.9	60.4	82.1
Aib13	30.5	41.3	68.1	91.7
Val15	59.5	75.8	59.5	75.8
Aib16	79.8	88.8	79.8	88.8

* Percentage of the trajectory during which the amide NH satisfies hydrogen bond criteria (NH···O dist. $\leq$2.7 or 3.0 Å; angle = 180 $\pm$ 60°) with α or 3_{10} carbonyl partners.

As *, but including G11-L9, V12-Q7, and Aib13-Aib8 percentage hydrogen bond lifetimes.

angles during the trajectories, similar to that illustrated in Fig. 1 for Aib13.

The P14 residue and the structural distortions around G11 result in some bending of the alamethicin structure. Defining this bending in terms of the angle between the helical segments N- and C-terminal to P14 is difficult because of the short length of the C-terminal helix and some perturbation of helix structure at the C-terminus during structural fluctuations. Where reliable measurements could be made, helix bend angles were between 170° (where 180° indicates that the helical segments N- and C-terminal to P14 are parallel) and ~120°. The intramolecular hydrogen bonds described above could be accommodated within this degree of helix bending; for example, the structures in Fig. 2 have helix bend angles of 146° (Fig. 2 *A*; x-ray crystal structure), 170° (Fig. 2 *B*), 123° (Fig. 2 *C*), and 125° (Fig. 2 *D*). To characterize helix bending more generally, we calculated the (all atom) molecular dipole of alamethicin in structures extracted from the dynamics trajectories. Using the partial charges in DISCOVER, the molecular dipole ranges from ~53 D in extended helical states to a minimum of ~31 D in the most bent states. (The dipole moments calculated using DISCOVER partial charges are somewhat lower (by ~15%) than those calculated by Sansom (1993, p. 394) using partial charges from the CHARMM force field.) State 1 structures always showed relatively little helix bending with generally high molecular dipole values. Although the molecular dipole was usually greater in conformational state 1 compared to states 2 and 3 (indicating greater helix bending in the latter cases), large molecular dipoles (low helix bending) were occasionally found in states 2 (Fig. 2 *B*) and 3. The partial reversal of the U10-G11 peptide bond (state 2; Fig. 3) in particular can be accommodated in a helical structure with a degree of bending similar to that found in the x-ray crystal structure (Fox and Richards, 1982), and with little perturbation of the helical hydrogen-bonded structure in adjacent residues. Similar rotation of the Thr11-Gly12 peptide bond of melittin is observed in methanol-solvated dynamics simulations from an α-helical starting structure (R. B. Sessions, N. Gibbs, and C. E. Dempsey, submitted). The structures with Aib13-Aib8 (π-helix) peptide bonds have a "looped out" appearance, apparent in the state 2 and 3 structures of Figs. 2 and 3. This looping out relieves close approaches between methylene or methyl side-chain groups of residue pairs P14 and Aib10, Aib13 and V9, and L12 and Aib8.

The bent structures observed in the simulations are different from those determined from simulated annealing calculations using NMR distance constraints in micelle-associated peptide (Franklin et al., 1994), although the region of structural variation responsible for helix bending (residues G11-Aib13) is the same. Bent states in the latter study are probably influenced by the lack of key NMR structural constraints, because bent structures were not positively defined by nuclear Overhauser effects, but resulted from structure calculations in which a small number of helix-defining nuclear Overhauser effects were absent. This is a significant problem in determining solution conformations of isolated helical peptides and is compounded in the case of alamethicin, with seven or eight Aib residues, for which stereochemical assignment of α-methyl resonances is not easily achieved. The bent states are also different from those observed in 100-ps solvent-free dynamics described by Fraternali (1990), although some similar hydrogen-bonding patterns (3_{10} hydrogen bonds and bifurcated hydrogen bonds involving L12 and V15 carbonyls) were found in that study.

CONCLUSIONS

Molecular dynamics simulations of alamethicin in methanol reproduce a number of structural features characterized spectroscopically, including the general stability of (helical) hydrogen-bonded secondary structure in that solvent with a well-defined pattern of α and 3_{10} hydrogen bonds. Several potentially contradictory pieces of spectroscopic evidence, the characterization of bent helical states (North et al., 1994) and of structural disorder around residues G11 to Aib13 (Yee et al., 1995), contrasting with high backbone order parameters (Kelsh et al., 1992) and stable hydrogen bonding for amide NHs (Dempsey, 1995), can be reconciled by comparison with the intrinsic structural preferences of the peptide found in the simulations. High helix stability is imparted by the presence of Aib residues, which resist deviation from helical geometry (Fig. 1). Helix stability may also result from the preference of intramolecular hydrogen bonds over peptide-solvent hydrogen bonds in methanol, because amide NHs in the structurally disordered states described here seek intramolecular hydrogen-bonding partners. Structural heterogeneity around Aib10-Aib13 is characterized by discrete structural states associated with well-defined flips of ϕ and ψ torsions involving the Aib10-G11 (and G11-L12) peptide bonds. Despite large deviations from helical hydrogen bond geometries, the amide NHs of G11, L12, and Aib13 can retain stable hydrogen bonding through the formation of nonregular hydrogen bonds (G11 NH-V9 CO, (L12 NH-Q7 CO), and Aib13 NH-Aib8 CO).

Thus the alamethicin structure can undergo significant modulation of the molecular dipole in nonaqueous environments by "flexing" around the peptide sequence before P14 while retaining stable hydrogen bonding. Although augmentation of the helix dipole does not fully account for the gating charge underlying voltage-dependent activation of ion conductance (Sansom, 1993), the conformational flexibility characterized in the spectroscopic studies and the simulations may contribute to channel gating, to the optimal orientation of the Aib10 and/or G11 carbonyl in solvating the channel lumen, or to channel noise (Mak and Webb, 1995). Because much of the flexibility involves reorientation of the Aib10-G11 peptide bond promoted by the lack of hydrogen bond constraints on Aib10 carbonyl and of a restricting side chain at residue 11, its contribution to the structural and functional properties of alamethicin might be investigated by analogs with substitutions (e.g., Gly to Ala) at residue 11. Both glycine and proline are abundant in known or predicted transmembrane helices of membrane transport proteins, and the motif x-G-X-P (melittin) or x-G-X-X-P (alamethicin) is also highly represented in these sequences (unpublished observations). Similar reversible reorientation of the respective x-G peptide bond in transmembrane helices of these proteins might be expected to occur and could play a functional role.

We are grateful to Andy Harvey, who helped with preliminary simulations.

Supported by grants from the Biotechnology and Biological Sciences Research Council (BBSRC) (GR/H36443), the Nuffield Foundation (SCI/180/91/46/G), and the Wellcome Trust. The BBSRC supports the Bristol Centre for Molecular Recognition.

REFERENCES

Baker, E. N., and R. E. Hubbard. 1984. Hydrogen-bonding in globular proteins. *Prog. Biophys. Mol. Biol.* 44:97–179.

Barlow, D. J., and J. Thornton. 1988. Helix geometry in proteins. *J. Mol. Biol.* 201:601–6019.

Brumfeld, V., and I. R. Miller. 1990. Electric-field dependence of alamethicin channels. *Biochim. Biophys. Acta* 1024:49–53.

Cafiso, D. S. 1994. Alamethicin—a peptide model for voltage gating and protein membrane interactions *Annu. Rev. Biophys. Biomol. Struct.* 23:141–165.

Dauber-Osguthorpe, P., V. A. Roberts, D. J. Osguthorpe, J. Wolff, M. Genest, and A. T. Hagler. 1988. Structure and energetics of ligand-binding to proteins: *Escherichia coli* dihydrofolate reductase trimethoprim, a drug-receptor system. *Proteins Struct. Funct. Genet.* 4:31–47.

Dempsey, C. E. 1995. Hydrogen bond stabilities in the isolated alamethicin helix: pH-dependent amide exchange measurements in methanol. *J. Am. Chem. Soc.* 117:7526–7534.

Dempsey, C. E., R. Bazzo, T. S. Harvey, I. Syperek, G. Boheim, and I. D. Campbell. 1991. Contribution of proline-14 to the structure and actions of melittin. *FEBS Lett.* 281:240–244.

Dempsey, C. E., and L. J. Handcock. 1996. Hydrogen bond stabilities in membrane-reconstituted alamethicin from amide-resolved hydrogen-exchange measurements. *Biophys. J.* 70:1777–1788.

Duclohier, H., G. Molle, J. Y. Dugast, and G. Spach. 1992. Prolines are not essential residues in the barrel-stave model for ion channels induced by alamethicin analogs. *Biophys. J.* 63:868–873.

Esposito, G., J. A. Carver, J. Boyd, and I. D. Campbell. 1987. High resolution ^{1}H NMR study of the solution structure of alamethicin. *Biochemistry.* 26:1043–1050.

Fox, R. O., and F. M. Richards. 1982. A voltage-gated ion channel model inferred from the crystal structure of alamethicin at 1.5 Å resolution. *Nature.* 300:325–330.

Franklin, J. C., J. F. Ellena, S. Jayasinghe, L. P. Kelsh, and D. S. Cafiso. 1994. Structure of micelle-associated alamethicin from ^{1}H NMR: evidence for conformational heterogeneity in a voltage-gated peptide. *Biochemistry.* 33:4036–4045.

Fraternali, F. 1990. Restrained and unrestrained molecular dynamics simulations in the NVT ensemble of alamethicin. *Biopolymers.* 30: 1083–1099.

He, K., S. J. Ludtke, D. L. Worcester, and H. W. Huang. 1996. Neutron-scattering in the plane of membranes: structure of alamethicin pores. *Biophys. J.* 70:2659–2666.

Kelsh, L. P., J. P. Ellena, and D. S. Cafiso. 1992. Determination of the molecular dynamics of alamethicin using ^{13}C NMR: implications for the mechanism of gating of a voltage-dependent channel. *Biochemistry.* 31:5136–5144.

Mak, D. D., and W. W. Webb. 1995. Molecular dynamics of alamethicin transmembrane channels from open-channel current noise analysis. *Biophys. J.* 69:2337–2349.

Marshall, G. R., E. E. Hodgkin, G. Langs, D. Smith, J. Zabrocki, and M. T. Leplawy. 1990. Factors governing helical preference of peptides containing multiple α,α-dialkyl amino acids. *Proc. Natl. Acad. Sci. USA.* 87:487–491.

North, C. L., M. Barranger-Mathys, and D. S. Cafiso. 1995. Membrane orientation of the N-terminal segment of alamethicin determined by solid-state ^{15}N NMR. *Biophys. J.* 69:2392–2397.

North, C. L., J. C. Franklin, R. G. Bryant, and D. S. Cafiso. 1994. Molecular flexibility demonstrated by paramagnetic enhancements of nuclear relaxation: application to alamethicin, a voltage-gated peptide channel. *Biophys. J.* 67:1861–1866.

Osguthorpe, D. J., and P. Dauber-Osguthorpe. 1992. FOCUS: a program for analyzing molecular dynamics simulations featuring digital signal-processing techniques. *J. Mol. Graphics.* 10:178–184.

Piela, L., G. Nemethy, and H. A. Scheraga. 1987. Proline-induced constraints in α-helices. *Biopolymers.* 26:1587–1600.

Rose, G. D., L. M. Gierasch, and J. A. Smith. 1985. Turns in peptides and proteins. *Adv. Protein Chem.* 37:1–109.

Sansom, M. S. P. 1993. Structure and function of channel-forming peptaibols. *Q. Rev. Biophys.* 26:365–421.

Sessions, R. B., P. Dauber-Osguthorpe, and D. J. Osguthorpe. 1989. Filtering molecular dynamics trajectories to reveal low-frequency collective motions: phospholipase A_2. *J. Mol. Biol.* 210:617–633.

Tauer, K. J., and W. N. Lipscomb. 1952. The crystal structure, residual entropy, and dielectric anomaly of methanol. *Acta Crystallogr.* 5:606–612.

Woolley, G. A., and B. A. Wallace. 1992. Model ion channels: gramicidin and alamethicin. *J. Membr. Biol.* 129:109–136.

Woolley, G. A., and B. A. Wallace. 1993. Temperature dependence of the interaction of alamethicin helices in membranes. *Biochemistry.* 32: 9819–9825.

Yee, A. A., R. Babiuk, and J. D. J. O' Neil. 1995. The conformation of an alamethicin in methanol by multinuclear NMR spectroscopy and distance geometry simulated annealing. *Biopolymers.* 36:781–792.

Yee, A. A., and J. D. J. O'Neil. 1992. Uniform ^{15}N labeling of a fungal peptide: the structure and dynamics of alamethicin by ^{15}N and ^{1}H NMR spectroscopy. *Biochemistry.* 31:3135–3143.

Yun, R. H., A. Anderson, and J. Hermans. 1991. Proline in α-helix stability and conformation studied by dynamics simulation. *Proteins.* 10: 219–228.

Zhang, L., and J. Hermans. 1994. 3_{10} helix versus α-helix: a molecular dynamics study of conformational preferences of Aib and alanine. *J. Am. Chem. Soc.* 116:11915–11921.